

# WZ Sge-type dwarf novae with multiple rebrightenings: MASTER OT J211258.65+242145.4 and MASTER OT J203749.39+552210.3

Chikako NAKATA,<sup>1\*</sup> Tomohito OHSHIMA,<sup>1</sup> Taichi KATO,<sup>1</sup> Daisaku NOGAMI,<sup>2</sup> Gianluca MASI,<sup>3</sup> Enrique de MIGUEL,<sup>4,5</sup> Joseph ULOWETZ,<sup>6</sup> Colin LITTLEFIELD,<sup>7</sup> William N. GOFF,<sup>8</sup> Thomas KRAJCI,<sup>9</sup> Hiroyuki MAEHARA,<sup>10</sup> William STEIN,<sup>11</sup> Richard SABO,<sup>12</sup> Ryo NOGUCHI,<sup>13</sup> Rikako ONO,<sup>13</sup> Miho KAWABATA,<sup>13</sup> Hisami FURUKAWA,<sup>13</sup> Katsura MATSUMOTO,<sup>13</sup> Takehiro ISHIBASHI,<sup>13</sup> Pavol A. DUBOVSKY,<sup>14</sup> Igor KUDZEJ,<sup>14</sup> Shawn DVORAK,<sup>15</sup> Franz-Josef HAMBSCH,<sup>16,17,18</sup> Roger D. PICKARD,<sup>19,20</sup> Etienne MORELLE,<sup>21</sup> Eddy MUJLLAERT,<sup>22</sup> Stefano PADOVAN,<sup>23</sup> Arne HENDEN,<sup>23</sup>

<sup>1</sup> Department of Astronomy, Kyoto University, Kyoto 606-8502

\*nakata@kusastro.kyoto-u.ac.jp

<sup>2</sup> Kwasan Observatory, Kyoto University, Yamashina, Kyoto 607-8471

<sup>3</sup> The Virtual Telescope Project, Via Madonna del Loco 47, 03023 Ceccano (FR), Italy

<sup>4</sup> Departamento de Física Aplicada, Facultad de Ciencias Experimentales, Universidad de Huelva, 21071 Huelva, Spain

<sup>5</sup> Center for Backyard Astrophysics, Observatorio del CIECEM, Parque Dunar, Matalascañas, 21760 Almonte, Huelva, Spain

<sup>6</sup> Center for Backyard Astrophysics Illinois, Northbrook Meadow Observatory, 855 Fair Ln, Northbrook, Illinois 60062, USA

<sup>7</sup> Department of Physics, University of Notre Dame, Notre Dame, Indiana 46556, USA

<sup>8</sup> 13508 Monitor Ln., Sutter Creek, California 95685, USA

<sup>9</sup> Astrokolkhoz Observatory, Center for Backyard Astrophysics New Mexico, PO Box 1351 Cloudcroft, New Mexico 83117, USA

<sup>10</sup> Kiso Observatory, Institute of Astronomy, School of Science, The University of Tokyo, 10762-30, Mitake, Kiso-machi, Kiso-gun, Nagano 397-0101, Japan

<sup>11</sup> 6025 Calle Paraiso, Las Cruces, New Mexico 88012, USA

<sup>12</sup> 2336 Trailcrest Dr., Bozeman, Montana 59718, USA

<sup>13</sup> Osaka Kyoiku University, 4-698-1 Asahigaoka, Osaka 582-8582

<sup>14</sup> Vihorlat Observatory, Mierova 4, Humenne, Slovakia

<sup>15</sup> Rolling Hills Observatory, 1643 Nightfall Drive, Clermont, Florida 34711, USA

<sup>16</sup> Groupe Européen d'Observations Stellaires (GEOS), 23 Parc de Levesville, 28300 Bailleau l'Évêque, France

<sup>17</sup> Bundesdeutsche Arbeitsgemeinschaft für Veränderliche Sterne (BAV), Munsterdamm 90, 12169 Berlin, Germany

<sup>18</sup> Vereniging Voor Sterrenkunde (VVS), Oude Bleken 12, 2400 Mol, Belgium

<sup>19</sup> The British Astronomical Association, Variable Star Section (BAA VSS), Burlington House, Piccadilly, London, W1J 0DU, UK

<sup>20</sup> 3 The Birches, Shobdon, Leominster, Herefordshire, HR6 9NG, UK

<sup>21</sup> 9 rue Vasco de GAMA, 59553 Lauwin Planque, France

<sup>22</sup> Vereniging Voor Sterrenkunde (VVS), Moffelstraat 13 3370 Boutersem, Belgium

<sup>23</sup> American Association of Variable Star Observers, 49 Bay State Rd., Cambridge, MA 02138, USA

(Received 201 0; accepted 201 0)

## Abstract

We report on photometric observations of WZ Sge-type dwarf novae, MASTER OT J211258.65+242145.4 and MASTER OT J203749.39+552210.3 which underwent outbursts in 2012. Early superhumps were recorded in both systems. During superoutburst plateau, ordinary superhumps with a period of 0.060291(4) d (MASTER J211258) and of 0.061307(9) d (MASTER J203749) in average were observed. MASTER J211258 and MASTER J203749 exhibited eight and more than four post-superoutburst rebrightenings, respectively. In the final part of the superoutburst, an increase in the superhump periods was seen in both systems. We have made a survey of WZ Sge-type dwarf novae with multiple rebrightenings, and confirmed that the superhump periods of WZ Sge-type dwarf novae with multiple rebrightenings were longer than those of WZ Sge-type dwarf novae without a rebrightening. Although WZ Sge-type dwarf novae with multiple rebrightenings have been thought to be the good candidates for period bouncers based on their low mass ratio ( $q$ ) from inferred from the period of fully grown (stage B) superhumps, our new method using the period of growing superhumps (stage A superhumps), however, implies higher  $q$  than those expected from stage B superhumps. These  $q$  values appear to be consistent with the duration of the stage A superoutbursts, which likely reflects the growth time of the 3:1 resonance. We present a working hypothesis that the small fractional superhump excesses for stage B superhumps in these systems may be explained as a result that a higher gas pressure effect works in these systems than in ordinary SU UMa-type dwarf novae. This result leads to a new picture that WZ Sge-type dwarf novae with multiple rebrightenings

and SU UMa-type dwarf novae without a rebrightening (they are not period bouncers) are located in the same place on the evolutionary track.

**Key words:** accretion, accretion disks — stars: novae, cataclysmic variables — stars: dwarf novae — stars: individual (MASTER OT J211258.65+242145.4, MASTER OT J203749.39+552210.3)

## 1. Introduction

Cataclysmic variables (CVs) are binary star systems that have a white dwarf (primary) and a secondary which fills its Roche lobe and transfers matter to the primary.

Dwarf novae (DNe) are one of subtypes of CVs. DNe have outbursts that are well understood as a release of gravitational energy caused by large mass transfer through the disk by the thermal instability. SU UMa-type dwarf novae are a subclass of DNe. They have occasional superoutbursts that are brighter and have longer durations than normal outbursts. During superoutbursts, they show light variations, which have a period few percent longer than the orbital period, called superhumps. It is believed that superhumps are caused by the tidal instability that is triggered when the disk radius expands to the critical radius for the 3:1 resonance [see e.g. Osaki (1996) for a theoretical review]. According to Kato et al. (2009a), SU UMa-type dwarf novae generally show three distinct stages of period variation of superhumps; the first stage with a longer superhump period (stage A), middle stage with systematically varying periods (stage B) and final stage with a shorter superhump period (stage C).

WZ Sge-type dwarf novae are a subgroup of dwarf novae [see e.g. Bailey 1979; Downes 1990; Kato et al. 2001]. They are known as systems that have infrequent large-amplitude superoutbursts. Although the general properties of outbursts in WZ Sge-type dwarf novae can be understood with thermal-tidal disk-instability model [see e.g. Osaki 1995, Osaki, Meyer (2003) for WZ Sge], there remain features in WZ Sge-type dwarf novae whose origin is still in dispute.

WZ Sge-type dwarf novae have several characteristic properties. One is the existence of double-wave early superhumps with periods close to the orbital periods in early stage of superoutbursts (Kato 2002). Patterson et al. (1981) originally suggested that these humps represent enhanced orbital humps arising from an enhanced mass transfer. Osaki, Meyer (2002) suggested that these humps arise from the 2:1 resonance. Although Patterson et al. (2002) now appears to favor the explanation by Osaki, Meyer (2002) for the origin of early superhumps, Patterson et al. (2002) suggested that an enhanced mass transfer plays a role in WZ Sge-type outbursts – post-superoutburst rebrightenings. Post-superoutburst rebrightenings [also called “echo outburst” by Patterson et al. (2002)] are often seen after superoutbursts of WZ Sge-type dwarf novae. These rebrightenings are classified by their morphology (Imada et al. 2006; Kato et al. 2009a). The mechanism of rebrightenings is still in dispute. There is a suggestion that the enhanced mass-transfer following the superoutburst cause rebrightenings (Hameury 2000; Buat-Ménard, Hameury 2002). On the

other hand, it is suggested that persistence of high viscosity in the accretion disk after the termination of the superoutburst produce rebrightenings (Osaki et al. 1997, Osaki et al. 2001). Patterson et al. (2002) wrote “hot-spot eclipses establish that mass transfer is greatly enhanced during superoutburst. This may settle the debate over the origin of echo outbursts in dwarf novae”, while Osaki, Meyer (2003) reported that the conclusion by Patterson et al. (2002) was a result of mis-interpretation of the observation, and there is no evidence of an enhanced mass transfer.

According to the standard evolutionary theory, CVs evolve from a longer to shorter orbital period and finally reach a minimum orbital period when the secondary begins to be degenerate or the thermal and mass-loss time scales become comparable for the secondary. Then the secondary becomes a brown dwarf which cannot remain in hydrogen burning or becomes somewhat oversized for its mass as a result of deviation from thermal equilibrium and the orbital period becomes longer again. The systems whose periods increase after reaching the minimum period are called period bouncers [see e.g. Knigge et al. (2011) for standard evolutionary theory of CVs]. A fraction of known WZ Sge-type dwarf novae are thought to be period bouncers because of their short orbital periods (Uemura et al. 2010; Patterson et al. 2005b; Patterson 2011).

Although the mechanism of rebrightenings are unknown, the rebrightenings have been thought to be related with evolutionary stages. Imada et al. (2006) and Kato et al. (2009a) classified the rebrightenings of WZ Sge-type dwarf novae into four types by their light curve shapes: long duration rebrightenings (type-A), multiple rebrightenings (type-B), single rebrightening (type-C), and no rebrightening (type-D). Kato et al. (2009a) indicated there is a relation between these rebrightening types and  $P_{\text{dot}}$  versus  $P_{\text{SH}}$  [see figure 37 of Kato et al. (2009a)]. This result implies that rebrightening type generally reflects the system parameters (the nature or the evolutionary state) of the system, although different superoutbursts in the same system sometimes show different rebrightening types [AL Com: Uemura et al. (2008); WZ Sge: Patterson et al. (1981)]. In EZ Lyn, however, two superoutbursts that have been observed so far were with type-B rebrightenings (Pavlenko et al. 2007; Kato et al. 2009b; Kato et al. 2012), suggesting that the same object tends to show the same type of rebrightenings. The cases were also true for UZ Boo (Kuulkers et al. 1996; Kato et al. 2009a) and WZ Sge (1978 and 2011, Patterson et al. 1981; Patterson et al. 2002; Ishioka et al. 2002c). We here assume as the starting point that WZ Sge-type dwarf novae can be generally categorized by the rebrightening type.

EG Cnc, one of WZ Sge-type dwarf novae, is known to have had a superoutburst with multiple rebrightenings

**Table 1.** Log of observations of MASTER J211258.

Start*	End*	mag <sup>†</sup>	error <sup>‡</sup>	$N^{\S}$	obs <sup>  </sup>	sys <sup>#</sup>
4.4570	4.5690	13.855	0.004	203	deM	C
4.5147	4.6119	13.815	0.002	308	Mas	C
4.6663	4.8883	13.584	0.002	235	UJH	C
4.6923	4.8649	13.698	0.003	96	BJA	V
4.6932	4.8818	13.907	0.001	664	LCO	C
4.7362	4.8962	13.891	0.001	287	SRI	C
4.7637	4.9541	13.902	0.001	458	SWI	V
5.3734	5.5402	13.544	0.001	419	DPV	C
5.4514	5.5950	13.998	0.001	483	Mas	C
5.6468	5.8412	14.061	0.001	425	LCO	C

\*BJD–2456100.

†Mean magnitude.

‡1- $\sigma$  of the mean magnitude.

§Number of observations.

||Observer’s code.

#Filter. “C” means no filter (clear).

(Patterson et al. 1998; Kato et al. 2004). It was discovered with its outbursts in 1977 by Huruhata (1983). Patterson et al. (1998) calculated its mass ratio  $q = 0.027$  from the fractional superhump excess, defined as  $\epsilon \equiv (P_{\text{sh}} - P_{\text{orb}})/P_{\text{orb}}$ . Using an average white dwarf mass of  $0.7 M_{\odot}$ , this suggests very low secondary mass  $M_2 \approx 0.02 M_{\odot}$ . After then, it has been generally considered that objects with multiple rebrightenings are good candidates of period bouncers.

In this paper, we present two WZ Sge-type dwarf novae which exhibited multiple rebrightenings. MASTER OT J211258.65+242145.4 was discovered by the Mobile Astronomical System of the Telescope-Robots (MASTER; Gorbovskoy et al. 2013) network (Denisenko et al. 2012, hereafter MASTER J211258). The quiescent counterpart was identified with a 20-th magnitude star. The large outburst amplitude ( $\sim 7$  mag) was suggestive of a WZ Sge-type dwarf nova (vsnet-alert 14697). MASTER OT J203749.39+552210.3 was discovered by MASTER network (Balanutsa et al. 2012, hereafter MASTER J203749). No previous outburst is known. The quiescent counterpart was identified with a 20-th magnitude star. The large outburst amplitude (more than 7 mag) was again suggestive of a WZ Sge-type dwarf nova. These objects turned out to be WZ Sge-type dwarf novae with multiple rebrightenings. We report in this paper on the development of their outbursts and superhumps and discuss the implications from the recorded variation of superhump periods. In Section 2, we briefly show a log of observations and the analysis method. In Section 3 and Section 4, we present the results of the observations of MASTER J211258 and MASTER J203749, respectively. In Section 5, we make a discussion on the results.

**Table 2.** Log of observations of MASTER J203749.

Start*	End*	mag <sup>†</sup>	error <sup>‡</sup>	$N^{\S}$	obs <sup>  </sup>	sys <sup>#</sup>
25.1165	25.2574	15.166	0.001	166	Mas	C
25.9345	26.1221	15.171	0.002	445	KU	C
25.9575	26.1298	15.236	0.003	441	Mhh	C
26.1294	26.3079	15.302	0.002	207	Mas	C
26.9299	27.1284	15.318	0.002	486	KU	C
28.2880	28.4762	15.308	0.002	240	deM	C
28.6062	28.7205	15.184	0.003	141	Kra	C
29.2833	29.4669	15.338	0.004	230	deM	C
29.5441	29.7184	15.247	0.004	167	Kra	C
29.9108	30.0583	15.270	0.005	304	KU	C
30.5411	30.7152	15.259	0.005	167	Kra	C
31.5406	31.7128	15.326	0.004	165	Kra	C
32.5403	32.7101	15.420	0.003	163	Kra	C
33.5390	33.7068	15.536	0.003	161	Kra	C
36.4837	36.6453	15.853	0.004	122	UJH	C
36.5406	36.6977	15.912	0.002	137	Kra	C
36.6880	36.8481	15.945	0.005	100	GFB	C
37.2884	37.3456	16.198	0.005	76	PXR	V
37.5412	37.6965	16.031	0.002	134	Kra	C
37.6903	37.8487	16.088	0.005	100	GFB	C
37.9127	38.1294	16.418	0.004	524	KU	C
38.5368	38.6939	16.851	0.007	136	Kra	C
38.9180	39.1222	18.341	0.021	500	KU	C
39.5366	39.6909	18.923	0.017	103	Kra	C
43.2612	43.2671	16.972	0.034	5	deM	C
43.5344	43.5405	16.414	0.013	5	Kra	C
43.7419	43.8332	16.395	0.005	58	GFB	C
44.2618	44.3051	16.866	0.007	30	deM	C
44.7044	44.8490	17.551	0.013	91	GFB	C
45.2640	45.2699	18.184	0.045	5	deM	C
45.6895	45.8433	18.768	0.033	86	GFB	C
46.6888	46.8426	16.502	0.006	96	GFB	C
50.2631	50.2720	17.189	0.016	7	deM	C
51.4569	51.4569	17.100	–	1	MUY	C
54.6967	54.8100	18.469	0.098	48	GFB	C
55.3672	55.3738	17.007	0.031	10	PXR	V
55.6799	55.8201	16.600	0.013	85	GFB	C
56.7061	56.8165	18.106	0.049	66	GFB	C
57.6870	57.8128	19.348	0.033	78	GFB	C

\*BJD–2456200.

†Mean magnitude.

‡1- $\sigma$  of the mean magnitude.

§Number of observations.

||Observer’s code.

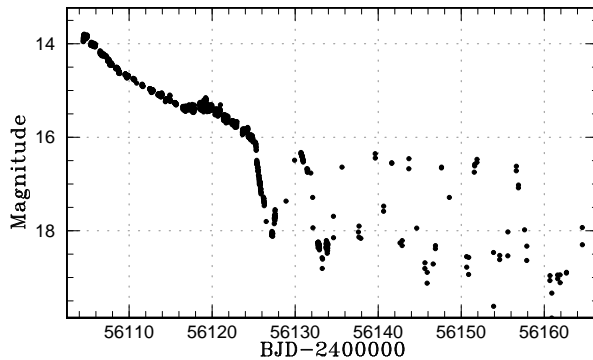
#Filter. “C” means no filter (clear).

**Table 4.** Comparison stars for MASTER J211258.

Observers	Comparison star
deM HMB	GSC 2186.232
Mhh	GSC 2190.396
OKU SWI DPV UJH	GSC 2190.309
OKU	GSC 2190.546

**Table 5.** Comparison stars for MASTER J203749.

Observers	Comparison star
deM Kra	GSC 3954.1468
KU	GSC 3954.649
Mhh	GSC 3954.2015

**Fig. 1.** Overall light curve of MASTER J211258. The data were binned to 0.01 d.

## 2. Observation and Analysis

The photometry log is given in tables 1 and 2. The continuation of table 1 can be seen on the electronic version. The observations are composed of those obtained by observers listed in table 3 and AAVSO observers. Comparison stars are shown in tables 4 and 5. The unfiltered CCD magnitudes are close to  $V$  for outbursting CVs.

All the observed times were corrected to barycentric Julian days (BJDs). The log of the observation is listed in table 2. Before making the analysis, we corrected zero-point differences between different observers by adding a constant to each observer.

In making period analysis, we used phase dispersion minimization (PDM) method (Stellingwerf 1978). We subtracted the global trend of the outburst light curve by subtracting smoothed light curve obtained by locally-weighted polynomial regression (LOWESS, Cleveland 1979) before making the PDM analysis. The  $1-\sigma$  error in periods of the PDM analysis was determined by the methods in Fernie (1989), Kato et al. (2010).

We used a variety of bootstrapping in estimating the robustness of the result of PDM. We typically analyzed 100 samples which randomly contain 50% of observations, and performed PDM analysis for these samples. The bootstrap result is shown as a form of 90% confidence intervals in the resultant  $\theta$  statistics.

## 3. MASTER OT J211258.65+242145.4

### 3.1. Overall Light Curve

Figure 1 shows the overall light curve of MASTER J211258. The object was first detected in superoutburst on June 24 (BJD 2456104). Although the early rise was hardly observed, the recorded possible maximum brightness of  $V = 13.72$  on about BJD 2456104.57 and the long duration of existence of early superhumps (subsection 3.2) suggest that the detection was made within a few days of the start of the superoutburst. The main superoutburst lasted until BJD 2456125, followed by a rapid decline. The object then faded below  $V = 18$ . On BJD 2456130, the first rebrightening ( $V = 16.32$  at maximum) was recorded.

Similar rebrightenings repetitively occurred eight times in total.

The light curve is composed of different segments: BJD 2456104–2456116, during which early superhumps were present, BJD 2456116–2456126, during which superhumps were present, and the following eight rebrightenings starting on BJD 2456130.

### 3.2. Early Superhumps

Since the orbital period is considered to be very close to the early superhump period (Ishioaka et al. 2002b), we used the period of the early superhump as the orbital period.

The early superhumps were fortunately well recorded. The doubly humped early superhumps with a period of 0.059732(3) d were recorded (figure 2) during the earliest 12 nights of observations. The mean amplitude of early superhumps was  $\sim 0.05$  mag. Figure 3 shows the nightly variation of the profile of early superhumps.

### 3.3. Ordinary Superhumps

The fractional superhump excess, an observational measure of the precession rate of the accretion disk, is defined by  $\epsilon$ , as mentioned in the introduction.

A period analysis indicated the presence of a very stable period of 0.060291(4) d during BJD 2456116–2456126 (figure 4). Figure 5 shows the nightly variation of the profile of ordinary superhumps. The amplitude of superhumps was 0.1–0.2 mag. They became larger until BJD 2456119, and then became smaller. The fractional superhump excess was 0.009376(7).

### 3.4. O – C Analysis of Ordinary Superhumps

We determined the times of maxima of ordinary superhumps in the way given in Kato et al. (2009a). The resultant times are listed in table 6.

The  $O - C$  curve of MASTER J2112 is shown in figure 6. The stage A ( $E \leq 38$ ) and stage B ( $E \geq 50$ ) are clearly seen. In stage A, superhumps have a long period and the period is decreasing. In stage B,  $P_{\text{dot}} (=P/P)$  is almost zero. The mean periods for these stages were 0.06158(5) d (stage A) and 0.060221(9) d (stage B), respectively.

**Table 3.** Observers and equipment.

Code *	Observer/Site	Equipment
Mas	G. Masi	43.2 cm telescope and STL6303E
deM	E. de Miguel	28cm telescope and QSI-518 wsg
UJH	J. Ulowetz	23.5cm telescope and QSI-583 wsg
LCO	C. Littlefield	-
KU	Kyoto University	40cm telescope and ST-9 CCD
GFB	W. Goff	-
Kra	T. Krajci	28cm telescope
Mhh	H. Maehara	25cm telescope and ST-7XME
SWI	W. Stein	35.56 cm telescope and ST10-XME
SRI	R. Sabo	-
OKU	Osaka Kyoiku U.	51cm telescope and ST-10 CCD
DPV	P. Dubovsky	28 cm telescope and Meade DSI ProII CCD 35.6 cm and Moravian Instruments G2-1600 CCD
DKS	S. Dvorak	-
HMB	F.-J. Hambusch	40cm telescope and FLI ML16803 CCD
PXR	R. Pickard	-
MEV	E. Morelle	-
PSD	S. Padovan	-
MUY	E. Muylaert	-

\*Observer's code used in table 1 and table 2.

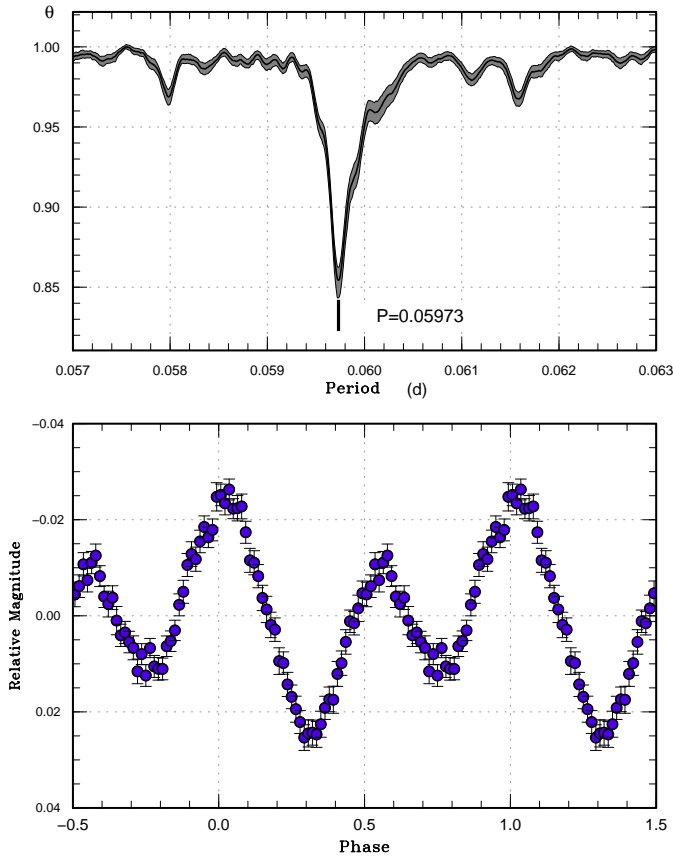


**Fig. 2.** Early superhumps in MASTER J211258 (BJD 2456104–2456116). (Upper): PDM analysis. (Lower): Phase-averaged profile.

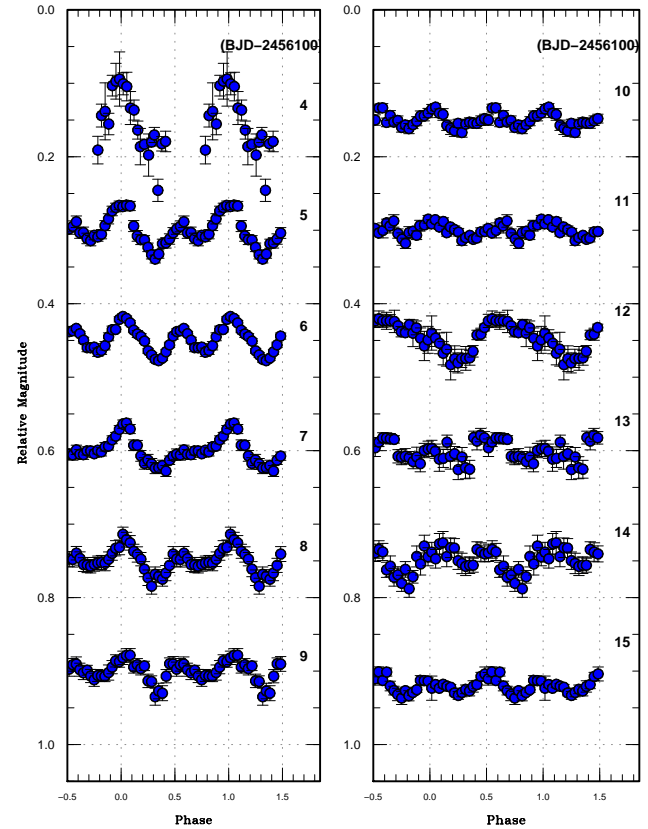


**Fig. 3.** Nightly variation of the profile of early superhumps in MASTER J211258.

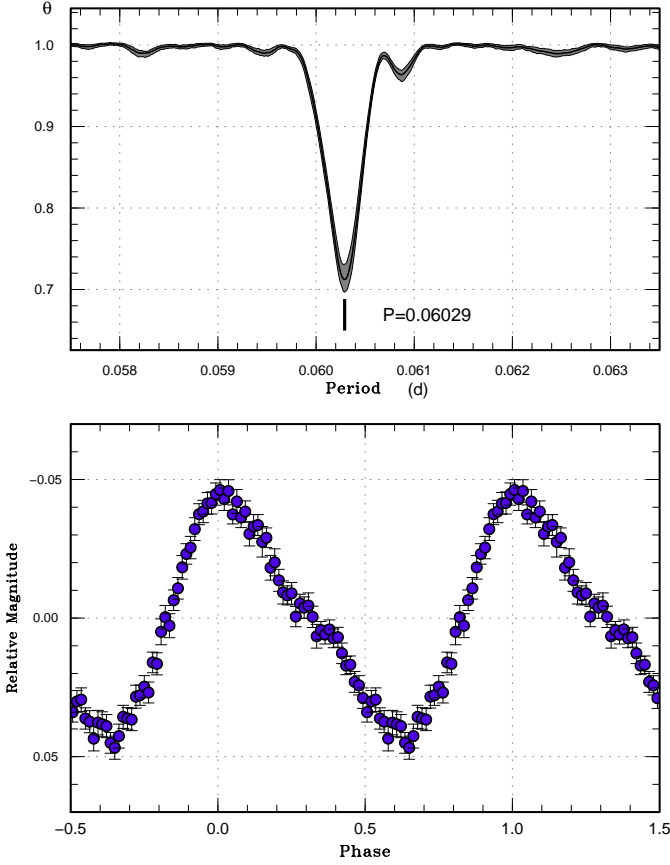


**Fig. 4.** Ordinary superhumps in MASTER J211258 (BJD 2456116–2456126). (Upper): PDM analysis. (Lower): Phase-averaged profile.

The  $P_{\text{dot}}$  for stage B ( $E \geq 50$ ) was  $+0.8(1.0) \times 10^{-5}$ . The peak of the superhump amplitudes is close to the time of stage A-B transition. A major increase in the period took place during the final part of stage B ( $E \geq 50$ ).

During stage A, superhumps with a period of 0.06158(5) d were observed and the fractional superhump excess was 0.0310(1).

#### 4. MASTER OT J203749.39+552210.3

##### 4.1. Overall Light Curve

Figure 7 shows the overall light curve of MASTER J203749. The object was first detected in superoutburst ( $V = 15.1$  at maximum) on October 22 (BJD 2456225). The short duration of the recorded early superhump stage suggests that the earlier part of the outburst was missed. The main superoutburst lasted until BJD 2456238, followed by a rapid decline. The object then faded below  $V = 19$ . On BJD 2456243, the first rebrightening ( $V = 16.37$  at maximum) was recorded. Similar rebrightenings repetitively occurred at least four times in total, although the number of observations was not sufficient to detect other potential rebrightenings.

The object developed early superhumps during BJD

**Table 6.** Times of superhump maxima in MASTER J211258.

$E$	maximum time*	error	$O - C^\dagger$	$N^\ddagger$
0	56115.5028	0.0025	-0.0382	66
1	56115.5607	0.0015	-0.0407	67
2	56115.6245	0.0016	-0.0372	59
16	56116.4927	0.0014	-0.0143	66
17	56116.5528	0.0012	-0.0146	66
18	56116.6204	0.0013	-0.0073	63
27	56117.1719	0.0012	0.0008	105
28	56117.2315	0.0011	0.0000	125
33	56117.5382	0.0005	0.0048	66
34	56117.5974	0.0005	0.0037	60
35	56117.6588	0.0005	0.0048	76
36	56117.7215	0.0009	0.0071	24
37	56117.7808	0.0010	0.0060	26
38	56117.8468	0.0022	0.0116	18
50	56118.5685	0.0003	0.0088	67
51	56118.6279	0.0004	0.0078	71
52	56118.6915	0.0012	0.0110	18
53	56118.7498	0.0006	0.0090	44
54	56118.8087	0.0005	0.0075	70
55	56118.8701	0.0006	0.0085	67
56	56118.9294	0.0008	0.0075	40
57	56118.9968	0.0019	0.0145	23
60	56119.1755	0.0013	0.0120	46
61	56119.2299	0.0007	0.0061	97
62	56119.2903	0.0013	0.0061	47
63	56119.3495	0.0025	0.0049	36
64	56119.4133	0.0003	0.0083	63
65	56119.4721	0.0004	0.0068	86
66	56119.5327	0.0004	0.0070	117
67	56119.5938	0.0005	0.0077	45
68	56119.6540	0.0005	0.0076	75
69	56119.7141	0.0011	0.0073	29
70	56119.7727	0.0005	0.0055	80
71	56119.8350	0.0006	0.0074	81
72	56119.8945	0.0007	0.0065	75
73	56119.9536	0.0006	0.0053	62
80	56120.3768	0.0006	0.0059	62
81	56120.4352	0.0005	0.0039	63
82	56120.4952	0.0004	0.0035	111
83	56120.5576	0.0005	0.0055	124
84	56120.6167	0.0007	0.0042	75
87	56120.7956	0.0006	0.0020	128
88	56120.8582	0.0008	0.0043	110
89	56120.9181	0.0007	0.0038	66
97	56121.3998	0.0005	0.0025	64
98	56121.4600	0.0005	0.0023	64
99	56121.5202	0.0005	0.0021	63
100	56121.5810	0.0004	0.0026	62
102	56121.6947	0.0034	-0.0044	16
103	56121.7615	0.0010	0.0020	80
104	56121.8205	0.0008	0.0006	129
105	56121.8848	0.0007	0.0045	132

\*BJD-2400000.

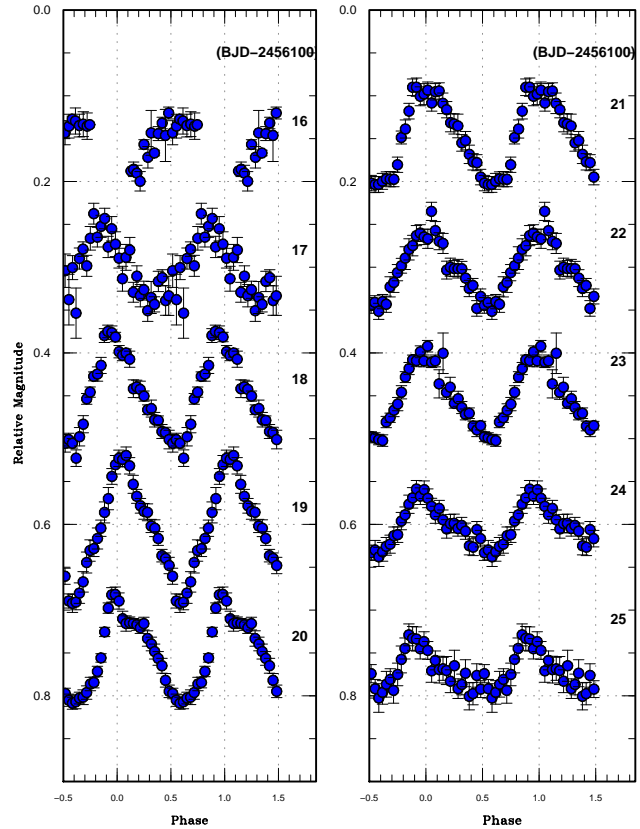
$^\dagger C = 2456115.5410 + 0.060375E$ .

$^\ddagger$ Number of points used to determine the maximum.

**Table 6.** Times of superhump maxima in MASTER J211258 (continued).

$E$	maximum time*	error	$O - C^\dagger$	$N^\ddagger$
113	56122.3643	0.0008	0.0010	49
114	56122.4239	0.0005	0.0003	64
115	56122.4819	0.0004	-0.0022	63
116	56122.5432	0.0007	-0.0012	44
120	56122.7844	0.0007	-0.0016	146
121	56122.8440	0.0007	-0.0023	148
122	56122.9054	0.0006	-0.0013	136
135	56123.6886	0.0010	-0.0029	83
136	56123.7474	0.0015	-0.0046	137
137	56123.8089	0.0009	-0.0034	169
138	56123.8698	0.0011	-0.0029	175
139	56123.9302	0.0016	-0.0029	66
145	56124.2904	0.0010	-0.0049	92
146	56124.3592	0.0037	0.0036	43
147	56124.4106	0.0009	-0.0055	52
148	56124.4721	0.0011	-0.0043	117
149	56124.5310	0.0007	-0.0058	102
150	56124.5881	0.0013	-0.0091	58
151	56124.6566	0.0058	-0.0009	58
152	56124.7135	0.0033	-0.0044	64
153	56124.7704	0.0026	-0.0079	64
154	56124.8337	0.0029	-0.0049	65
155	56124.8888	0.0026	-0.0102	72
161	56125.2584	0.0007	-0.0028	66
163	56125.3804	0.0010	-0.0016	43
164	56125.4347	0.0010	-0.0077	59
165	56125.4960	0.0014	-0.0068	88
166	56125.5565	0.0012	-0.0067	83
167	56125.6205	0.0021	-0.0030	65
169	56125.7410	0.0044	-0.0033	20
170	56125.7947	0.0033	-0.0100	29
171	56125.8617	0.0061	-0.0034	23
177	56126.2210	0.0012	-0.0063	66
178	56126.2866	0.0018	-0.0010	49
193	56127.2114	0.0016	0.0181	66
194	56127.2615	0.0025	0.0078	66

\*BJD-2400000.

 $^\dagger C = 2456115.5410 + 0.060375E$ . $^\ddagger$ Number of points used to determine the maximum.**Fig. 5.** Nightly variation of the profile of ordinary superhumps in MASTER J211258.

2456225–2456227. During BJD 2456227–2456238, superhumps appeared.

#### 4.2. Early Superhumps

It was likely that the final stage of early superhumps was observed. The mean period of 0.06051(18) d was recorded during BJD 2456225–2456227 (figure 8). We identified this period to be the orbital period. Figure 9 shows the nightly variation of the profile of early superhumps. The data give a larger error than in MASTER J211258 because a period of the observations was short than in MASTER J211258.

#### 4.3. Ordinary Superhumps

Ordinary superhumps with a period of 0.061307(9) d developed during BJD 2456227–2456238 (figure 10). Figure 11 shows the nightly variation of the profile of ordinary superhumps. The growth of ordinary superhumps was clearly seen. The amplitude increased until around BJD 2456231, and then became smaller. The fractional superhump excess was 0.01334(15).

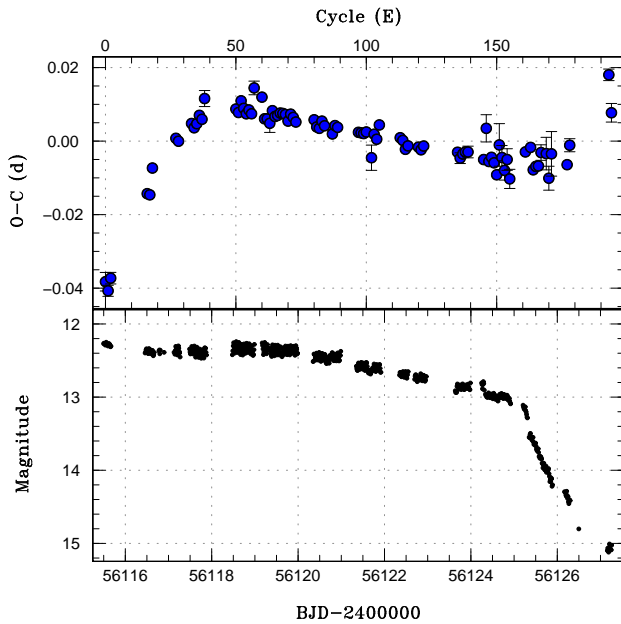


**Fig. 6.** The  $O - C$  curve of MASTER J211258 during the superoutburst. (Upper:)  $O - C$  diagram of superhumps in MASTER J211258. An ephemeris of BJD  $2456115.541 + 0.060375E$  was used to draw this figure. (Lower:) Light curve. The data were binned to 0.01 d.

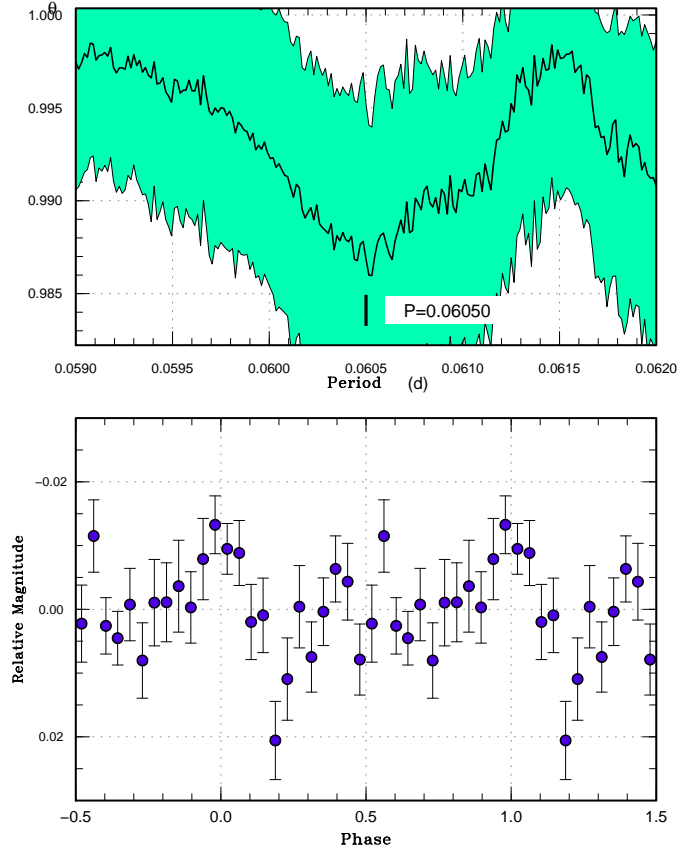


**Fig. 8.** Early superhumps in MASTER J203749 (BJD  $2456225 - 2456227$ ). (Upper:) PDM analysis. (Lower:) Phase-averaged profile.

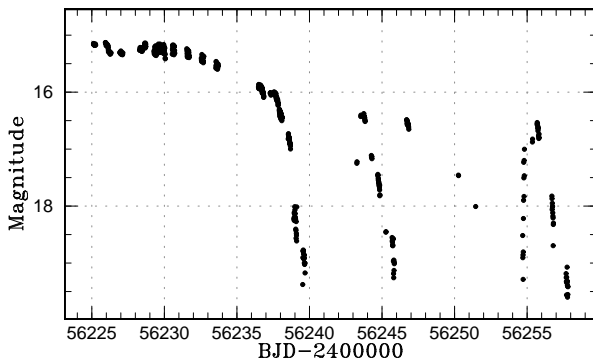


**Fig. 7.** Overall light curve of MASTER J203749. The data were binned to 0.01 d.

#### 4.4. $O - C$ Analysis of Ordinary Superhumps

The times of superhump maxima are listed in table 7. The  $O - C$  curve of MASTER OT J2037 is shown in figure 12, clearly composed of stages A ( $E \leq 30$ ) and B ( $E \geq 36$ ). The mean periods for these stages were 0.06271(11) d (stage A) and 0.061307(9) d (stage B), respectively.

Disregarding stage A superhumps ( $E \leq 30$ ), a marginally positive  $P_{\text{dot}}$  of  $+2.9(1.0) \times 10^{-5}$  was recorded. A major increase in the period also took place during the final part of stage B ( $E \geq 36$ ).

During stage A, superhumps with a period of 0.06271(11) d were recorded and the fractional superhump excess was 0.0365(2).

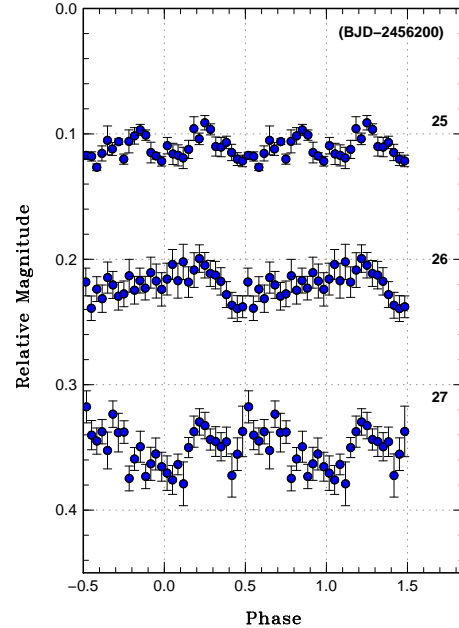
The analysis showed  $P_{\text{dot}}$  during stage B of both MASTER J211258 and MASTER J203749 were positive. The positive period derivatives were reported in some dwarf novae including WZ Sge-type dwarf novae. The mechanism that causes positive period derivatives of superhump periods is unknown.



**Table 7.** Times of superhump maxima in MASTER J203749.

$E$	maximum time*	error	$O - C^\dagger$	$N^\ddagger$
0	56228.33	0.0012	-0.0186	62
1	56228.39	0.0013	-0.0168	62
2	56228.46	0.0014	-0.0134	54
5	56228.64	0.0006	-0.0146	60
6	56228.70	0.0007	-0.0122	51
15	56229.28	0.0050	0.0095	23
16	56229.33	0.0006	0.0030	59
17	56229.39	0.0005	0.0037	62
18	56229.46	0.0006	0.0054	44
20	56229.58	0.0003	0.0063	47
21	56229.64	0.0003	0.0062	47
22	56229.70	0.0006	0.0049	37
26	56229.95	0.0006	0.0079	125
27	56230.01	0.0025	0.0005	75
36	56230.57	0.0003	0.0080	46
37	56230.63	0.0003	0.0082	47
38	56230.69	0.0003	0.0074	47
52	56231.55	0.0011	0.0046	27
53	56231.61	0.0004	0.0073	47
54	56231.67	0.0006	0.0077	47
68	56232.53	0.0032	0.0076	15
69	56232.59	0.0005	0.0011	47
70	56232.65	0.0006	0.0014	47
71	56232.71	0.0010	0.0019	26
85	56233.57	0.0004	0.0010	47
86	56233.63	0.0005	0.0004	47
87	56233.69	0.0007	-0.0018	41
133	56236.51	0.0017	-0.0043	35
134	56236.57	0.0009	-0.0016	80
135	56236.64	0.0012	-0.0015	70
136	56236.69	0.0014	-0.0063	46
137	56236.76	0.0008	-0.0051	30
138	56236.81	0.0019	-0.0076	32
150	56237.55	0.0014	-0.0048	32
151	56237.62	0.0011	-0.0034	42
152	56237.68	0.0010	-0.0034	46
153	56237.74	0.0015	-0.0050	29
154	56237.80	0.0015	-0.0031	32
156	56237.92	0.0023	-0.0049	82
157	56237.99	0.0019	-0.0033	104
158	56238.06	0.0038	0.0062	118
159	56238.12	0.0035	0.0048	95
166	56238.55	0.0009	0.0116	34
167	56238.61	0.0016	0.0022	43
168	56238.67	0.0023	0.0019	42
173	56238.99	0.0028	0.0141	121
175	56239.09	0.0039	-0.0079	121
183	56239.58	0.0034	-0.0078	32
184	56239.65	0.0059	0.0023	32

\*BJD-2400000.

 $^\dagger C = 2456228.358 + 0.060135E$ . $^\ddagger$ Number of points used to determine the maximum.**Fig. 9.** Nightly variation of the profile of early superhumps in MASTER J203749.

## 5. Discussion

### 5.1. Brightening Associated with Evolution of Ordinary Superhumps

In MASTER J211258, a sudden increase of the system brightness took place during the evolutionary stage of ordinary superhumps (BJD 2456116–2456118). In MASTER J203749, a possible increase of brightening was seen around BJD 2456229.5–2456230.

This phenomenon is naturally explained by the increase of dissipation rate as a result of the growth of tidal instability.

The systems with an increase of brightening during the evolutionary stage of ordinary superhumps are listed in table 8. We can see a possible tendency that these systems exhibit long rebrightening or multiple rebrightenings.

### 5.2. Duration of the Stage A Superhumps

The stage A superhumps had been observed for about three days in both MASTER J211258 and MASTER J203749.

The duration of the stage A (growing stage of the superhumps) is expected to be a good measure for the growth time of the 3:1 resonance. The growth rate of the 3:1 resonance is shown to be proportional to  $q^2$  (Lubow 1991), and a longer stage A is expected for a low  $q$  system. This has recently been confirmed in a likely period bouncer ( $q \lesssim 0.05$ ) SSS J122221.7–311523, which showed a duration of stage A amounting to 11–15 d (Kato et al. 2013b).

Although Patterson et al. (1998) estimated the mass ratio of EG Cnc to be  $q = 0.027$ , this value might be

**Table 8.** The systems with the increase of brightening during evolutionary stage of ordinary superhumps.

Object	Year	Rebrightening*	Reference
V466 And	2008	A	Kato et al. (2009a)
NN Cam <sup>†</sup>	2009	-	Kato et al. (2010)
EG Cnc	1996	B	Patterson et al. (1998)
AL Com	1995	A	Nogami et al. (1997), Patterson et al. (1996), Kato et al. (2009a)
V592 Her <sup>†</sup>	2010	-	Kato et al. (2009a)
EZ Lyn	2010	B	Kato et al. (2012)
WZ Sge	2001	A	Ishioka et al. (2002a), Kato et al. (2009a)

\*Classification of the rebrightenings of WZ Sge-type stars (subsection 5.6).

<sup>†</sup>Possible increase.

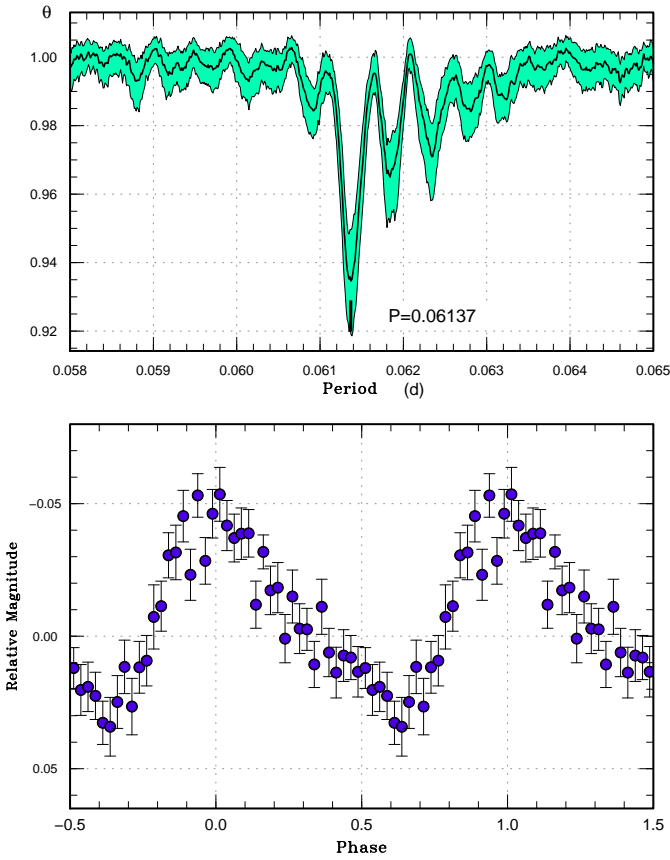


**Fig. 10.** Ordinary superhumps in MASTER J203749 (BJD 2456227–2456238). (Upper): PDM analysis. (Lower): Phase-averaged profile.

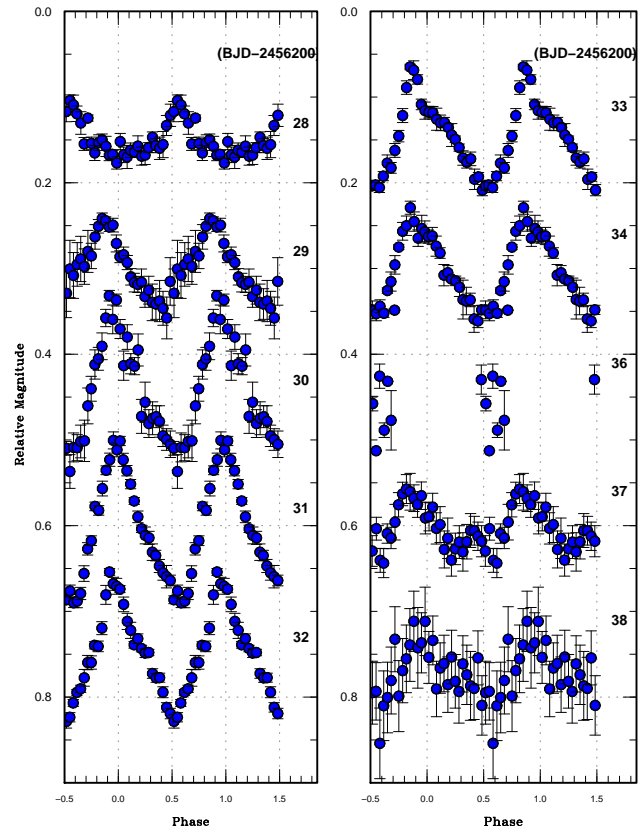


**Fig. 11.** Nightly variation of the profile of ordinary superhumps in MASTER J203749.

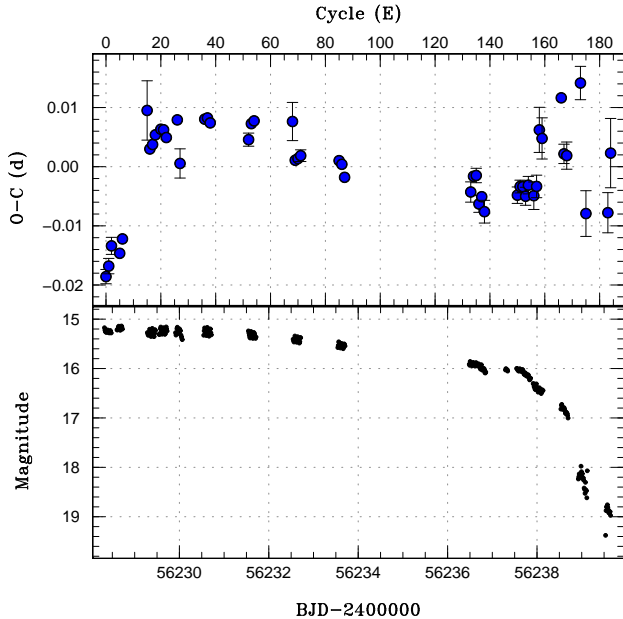


**Fig. 12.** The  $O - C$  curve of MASTER J203749 during the superoutburst. (Upper:)  $O - C$  diagram of superhumps in MASTER J203749. An ephemeris of BJD  $2456228.358 + 0.060135E$  was used to draw this figure. (Lower:) Light curve. The data were binned to 0.01 d.

significantly too small for its short duration of stage A superhumps (stage A superhumps were not identified in this object; we estimated the duration of stage A to be less than 3 d from the epochs of early superhumps and fully grown superhumps). We propose that  $q$  of EG Cnc should be re-examined.

### 5.3. Mass-Ratio from Stage A Superhumps

Quite recently, Osaki, Kato (2013), proposed an important interpretation: the dynamical precession rate at the 3:1 resonance is represented in the growing stage of superhumps (stage A) when the eccentric wave is still confined to the location of the resonance. Kato, Osaki (2013) systematically studied stage A superhumps in SU UMa-type dwarf novae and confirmed that the mass ratios determined from fractional superhump excesses of stage A superhumps are in good agreement with those determined from quiescent eclipse observations or radial-velocity study. Kato, Osaki (2013) also confirmed that the evolutionary sequence using these mass ratios is in good agreement with the most recent evolutionary sequence determined from modern precise eclipse observations [such as Littlefair et al. (2008)]. Having the theoretical background (Osaki, Kato 2013), we used this relation to estimate the mass ratio.

This relation gives mass ratios of MASTER J211258 and MASTER J203749  $q = 0.081(2)$  and  $q = 0.097(8)$  respectively.

The traditional method to estimate mass ratios from

fractional superhump excesses of stage B superhumps, using

$$\epsilon = 0.16(2)q + 0.25(7)q^2 \quad (1)$$

(Kato et al. 2009a) or

$$\epsilon = 0.18q + 0.29q^2 \quad (2)$$

(Patterson et al. 2005a), gives mass ratios of MASTER J211258 and MASTER J203749  $q = 0.054$  and  $q = 0.080$ , respectively.

The mass ratios from stage A superhumps are higher than the mass ratios from stage B superhumps. This discrepancy will be discussed in subsection 5.7.

### 5.4. Duration of the Early Superhump Stage

The early superhumps were observed for 12 d in MASTER J211258 and for 3 d in MASTER J203749 (we must note that MASTER J203749 was not detected sufficiently early, and this duration is a lower limit of the actual duration). Table 9 shows the duration of the early superhump stage of well-observed WZ Sge-type dwarf novae.

Early superhumps are thought to be a manifestation of the 2:1 resonance (Osaki, Meyer 2002). During the stage of early superhumps, the 2:1 resonance is dominant since the development of the 2:1 resonance is expected to suppress the 3:1 resonance (Lubow 1991, Osaki, Meyer 2003). Therefore the duration of the early superhump stage is expected to be dependent on the disk mass at beginning of the outburst and the disk radius of 2:1 resonance relative to the Roche lobe. It is expected that small  $q$  and large disk mass lead to long duration of the early superhump stage because the disk radius of 2:1 resonance is related to  $q$ .

In EG Cnc, this picture suggests that the comparatively short duration (less than 10 d, even if we consider the maximum duration of the observational gap) of the early superhump stage appears to be incompatible with the very small mass ratio  $q = 0.027$  estimated by Patterson et al. (1998). Either actual  $q$  may be larger or the disk mass of EG Cnc at the start of the superoutburst may have been exceptionally small.

### 5.5. Period in Post-Superoutburst State

During final part of the superoutburst, an increase in the superhump period was seen both in MASTER J211258 and MASTER J203749. The tendency is similar to that of EZ Lyn, the eclipsing WZ Sge-type dwarf nova with multiple rebrightenings (Kato et al. 2012). The  $O - C$  diagram of EZ Lyn is shown in figure 13.

Lubow (1992) suggested that disk precession is due to a combination of effects of direct axisymmetric tidal forces from secondary, which is the most important, gas pressure in the eccentric mode and resonant wave stresses. Pressure forces act to decrease the precession rate. The tidal effect dominates for superhump binaries and produces a net prograde precession. The gas pressure effect produces a retrograde contribution and decrease the precession rate. The inward propagation of the eccentricity

**Table 9.** Duration of the early superhump stage.

Object	Year	Duration*	References
EG Cnc	1996	2–10	Matsumoto, Schmeer (1996)
ASAS J0233	2006	8	Kato et al. (2009a)
V455 And	2007	7	Kato et al. (2009a)
V466 And	2008	11	Kato et al. (2009a)
AL Com	1995	5	Kato et al. (1996)
DV Dra	2005	]5 <sup>†</sup>	Kato et al. (2009a)
BW Scl	2011	10	Kato et al. (2013a)
WZ Sge	2001	11	Ishioka et al. (2002c)
OT J0120	2010	11	Kato et al. (2010)

\*Unit d.

†”]” represents the lower limit.

wave is accompanied by an increase of the pressure effect. Therefore the pressure effect is larger in stage B than in stage A. Furthermore, it is expected that the decrease in the pressure effect due to the transition to a cool state leads to the increase in the precession rate during final part of the superoutburst, which results in the increase in the superhump period. The increase in the period in MASTER J211258 and MASTER J203749 during the final part of superoutburst is exactly what is expected for this interpretation.

From Kato, Osaki (2013), Kato et al. (2013b), the fractional superhump excesses (in frequency unit) of the stage A and post-superoutburst superhumps are expressed as follows:

$$\epsilon^*(\text{post}) = Q(q)R(r_{\text{post}}) \quad (3)$$

and

$$\epsilon^*(\text{stageA}) = Q(q)R(r_{3:1}), \quad (4)$$

where  $r_{3:1}$  is the radius of 3:1 resonance

$$r_{3:1} = 3^{(-2/3)}(1+q)^{-1/3}. \quad (5)$$

$\epsilon^* \equiv 1 - P_{\text{orb}}/P_{\text{SH}}$ ,  $r_{\text{post}}$  is the dimensionless disk radius immediately after the outburst measured in units of binary separation  $A$ ,

$$Q(q) = \frac{1}{2} \frac{q}{\sqrt{1+q}}, \quad (6)$$

and

$$R(r) = \frac{1}{2} \frac{1}{\sqrt{r}} b_{3/2}^{(1)}(r), \quad (7)$$

where  $\frac{1}{2}b_{s/2}^{(j)}$  is the Laplace coefficient

$$\frac{1}{2}b_{s/2}^{(j)}(r) = \frac{1}{2\pi} \int_0^{2\pi} \frac{\cos(j\phi)d\phi}{(1+r^2-2r\cos\phi)^{s/2}}. \quad (8)$$

Using the relation as follows:

$$\frac{\epsilon^*(\text{stageA})}{\epsilon^*(\text{post})} = \frac{R(r_{3:1})}{R(r_{\text{post}})} \quad (9)$$

we can obtain  $R(r_{\text{post}})$ . In MASTER J211258, post-superoutburst superhumps with a period of 0.06050(6) d

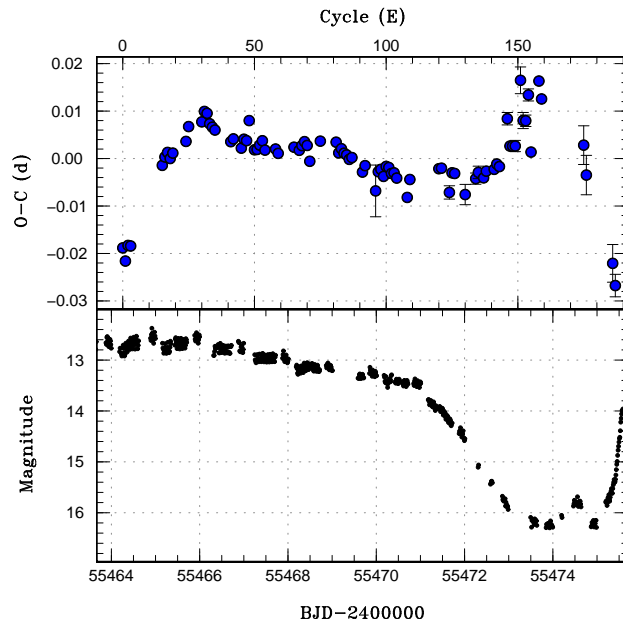


**Fig. 13.** The  $O - C$  curve of EZ Lyn during the superoutburst [the data are taken from Kato et al. (2012)]. (Upper:)  $O - C$  diagram of superhumps in EZ Lyn. An ephemeris of BJD 2455464.258+0.05966E was used to draw this figure. (Lower:) Light curve. The data were binned to 0.01 d.

were recorded in the final part of the superoutburst (BJD 2456124.5–2456126.5). The equation (3) gives  $r = 0.33$  using  $q$  from stage A superhump. Kato et al. (2013) showed  $0.30 \leq r \leq 0.38$  for the post-superoutburst state of WZ Sge-type dwarf novae. The agreement appears to be good.

### 5.6. Post-Superoutburst Rebrightenings

The rebrightenings of MASTER J211258 are considered to be type-B rebrightenings based on the classification by Imada et al. (2006). Figure 14 shows  $P_{\text{dot}}$  versus  $P_{\text{SH}}$ , including the data reported in Kato et al. (2009a) and Nakagawa et al. (2013). The filled circles, filled squares, filled triangles, and open circles represent type-A, type-

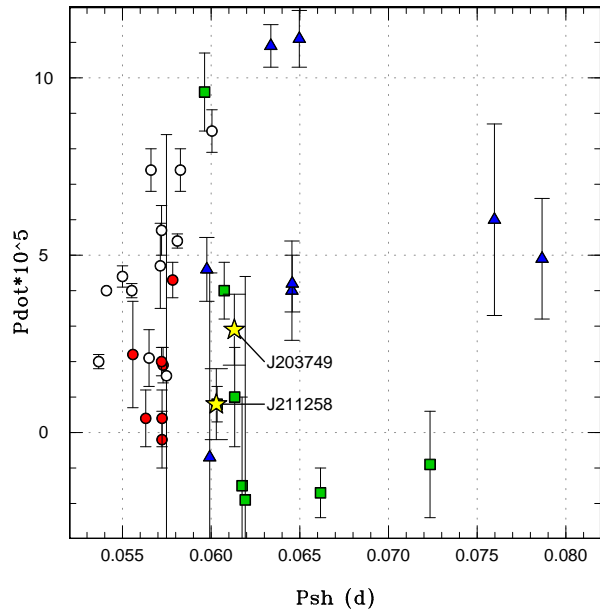


**Fig. 14.**  $P_{SH}$  versus  $P_{dot}$  for each type of rebrightenings. The star marks represent the two MASTER objects studied in this work. The other data are from Kato et al. (2009a). The filled circles, filled squares, filled triangles, and open circles represent type-A, type-B, type-C and type-D, respectively.

B, type-C and type-D, respectively (these points represent different outbursts; we hereafter call them “type-X object” assuming that the outburst type generally represents the property of the object). The locations of MASTER J211258 and MASTER J203749, expressed by filled stars, indicate that they are located close to the known type-B objects.

Table 10 and 11 list WZ Sge-type dwarf novae with multiple rebrightenings and those without a rebrightening, respectively. Although two systems (QZ Ser and OGLE-GD-DN-014) with longer superhump periods ( $\geq 0.07$  d) and multiple rebrightenings have been reported, at least one of them (QZ Ser) is an object which is not on the standard evolutionary track (Ohshima et al in prep.; Thorstensen et al. 2002). We therefore disregard the systems with longer superhump periods in table 10.

Figure 15 shows a cumulative frequency of the distribution of superhump periods. Solid and dashed line represent type-B and type-D objects, respectively.

The Kolmogorov-Smirnov test shows that the superhump periods distribution of type-D (no rebrightening) and type-B (multiple rebrightenings) do not belong to the same parent population with a significance level of  $p < 0.001$ . We can safely conclude that the superhump periods of type-B objects are longer than those of type-D objects.

**Table 10.** WZ Sge-type dwarf novae with multiple rebrightenings. The data are from Kato et al. (2009a), Kato et al. (2012), Kato et al. (2013a) and Mroz et al. (2013).

Object	Year	$N_{reb}^*$	$P_{SH}$
UZ Boo	1994	2:	0.061743(38)
UZ Boo	2003	4	0.061922(33)
DY CMi	2008	6	0.060736(9)
EG Cnc	1996	6	0.060337(6)
AL Com	2008	$4^\dagger$	0.057174(6)
VX For	2009	5	0.061327(12)
EZ Lyn	2006	11	0.059537(31)
EZ Lyn	2010	6	0.059630(16)
EL UMa	2010	$4^\dagger$	0.06045(6) $^\ddagger$
1RXS J0232	2007	4	0.066166(11)
OGLE-GD-DN-001	2007	4	0.06072(2)
MASTER J2037	2012	$3^\dagger$	0.061307(9)
MASTER J2112	2012	8	0.060291(4)

\*Number of rebrightenings.

$^\dagger$ ]” represents the lower limit.

$^\ddagger$ During the rebrightening phase.

**Table 11.** WZ Sge-type dwarf novae without a rebrightening.

Object	Year	$P_{SH}$
SV Ari	2011	0.055524(14)
V455 And	2007	0.057133(10)
V466 And	2008	0.057203(15)
V592 Her	1998	0.056498(13)
V592 Her	2010	0.056607(16)
V1108 Her	2004	0.057480(34)
GW Lib	2007	0.054095(10)
BW Scl	2011	0.055000(8)
HV Vir	2002	0.058266(17)
SDSS J1339	2011	0.058094(7)
OT J0238	2008	0.053658(7)
OT J2138	2010	0.055019(12)
OT J2109	2011	0.060045(26)

**Table 13.** Fractional superhump excesses (in frequency unit) from stage A superhumps for SU UMa-type dwarf novae without a rebrightening with the period range of 0.05875–0.06458 d.

Object	$P_{orb}^\ddagger$	$P_{SH}^\ddagger$ (stage A)	$\epsilon^* \dagger$
V1040 Cen	0.06030	0.06243(6)	0.0341(10)
WX Cet	0.05826	0.06029(8)	0.0336(14)
PU CMa	0.05669	0.05901(21)	0.0392(37)
MM Hya	0.05759	0.06163(24)	0.0656(42)
SW UMa	0.05681	0.05893(8)	0.0360(14)
SDSS J1610	0.05687	0.05881(9)	0.0330(16)
OT J1044	0.05909	0.06084(2)	0.0287(3)
OT J2109	0.05865	0.06087(6)	0.0364(10)

$^\ddagger$ Unit d.

$^\dagger$ Fractional superhump excess (in frequency unit).

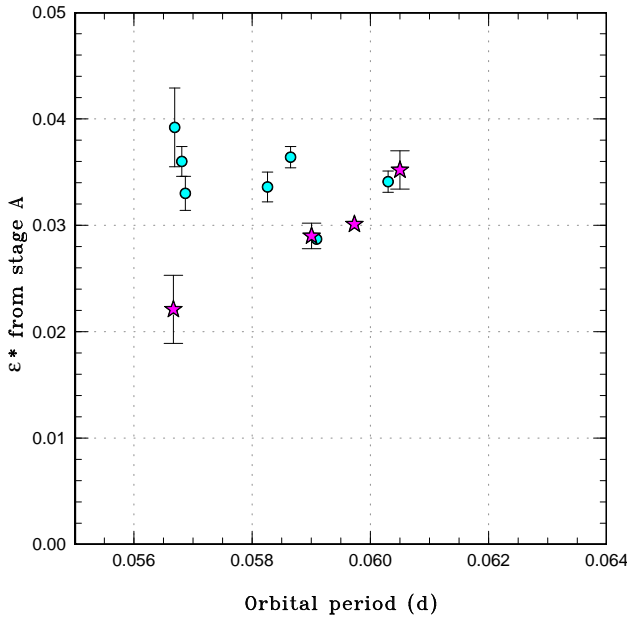


**Fig. 16.**  $P_{\text{orb}}$  versus  $\epsilon^*$  for stage A superhumps. The data are from our result, Kato et al. (2009a), Kato et al. (2012), and Kato et al. (2013a). Filled circles and filled stars represent SU UMa-type dwarf novae without a rebrightening and WZ Sge-type dwarf novae with multiple rebrightenings, respectively.

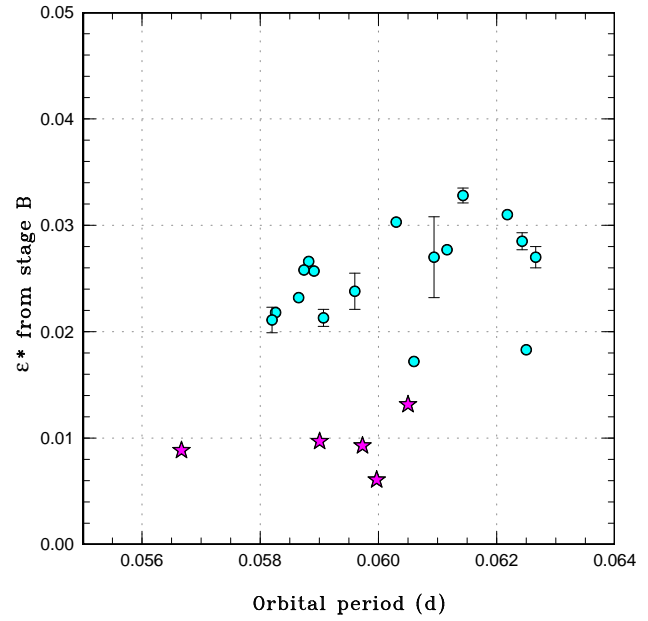


**Fig. 17.**  $P_{\text{orb}}$  versus  $\epsilon^*$  for stage B superhumps. The data are from our result, Kato et al. (2009a), Kato et al. (2012), and Kato et al. (2013a). Filled circles and filled stars represent SU UMa-type dwarf novae without a rebrightening and WZ Sge-type dwarf novae with multiple rebrightenings, respectively.

**Table 12.** Fractional superhump excesses (in frequency unit) of WZ Sge-type dwarf novae with multiple rebrightenings.

Object	$P_{\text{orb}}^{\ddagger}$	$P_{\text{SH}}^{\ddagger}(\text{stage B})$	$\epsilon^{*\ddagger}(\text{stage B})$	$P_{\text{SH}}^{\ddagger}(\text{stage A})$	$\epsilon^{*\ddagger}(\text{stage A})$
UZ Boo	-	0.061831(36)	-	0.06354(24)	-
DY CMi	-	0.060736(9)	-	-	-
EG Cnc	0.05997	0.060337(6)	0.00608(10)	-	-
AL Com	0.056668	0.057174(6)	0.00885(11)	0.05795(18)	0.0221(32)
VX For	-	0.061327(12)	-	-	-
EZ Lyn	0.059005	0.059584(24)	0.00970(41)	0.06077(7)	0.0290(12)
1RXS J0232	-	0.066166(11)	-	-	-
MASTER J2037	0.06051	0.061307(9)	0.01316(15)	0.06271(11)	0.0352(18)
MASTER J2112	0.05973	0.06029(4)	0.00929(67)	0.06158(5)	0.0301(8)

$\ddagger$ Unit d.

$\ddagger$ Fractional superhump excess (in frequency unit).

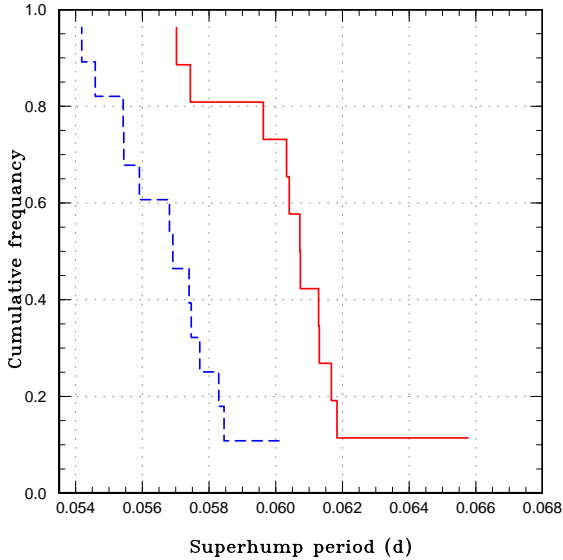


**Fig. 15.** Cumulative frequency of the distribution of superhump periods of WZ Sge-type stars with multiple rebrightenings (type-B) and those without a rebrightening (type-D). Solid and dashed line indicate that of type-B objects and type-D objects, respectively.

**Table 14.** Fractional superhump excesses (in frequency unit) from stage B superhumps for SU UMa-type dwarf novae without a rebrightening with the period range of 0.05875–0.06458 d.

Object	$P_{\text{orb}}^{\ddagger}$	$P_{\text{SH}}^{\ddagger}$ (stage B)	$\epsilon^*$ $\dagger$
NZ Boo	0.05891	0.06046(1)	0.0257(2)
V436 Cen	0.06250	0.06366(1)	0.0183(2)
V1040 Cen	0.06030	0.06218(3)	0.0303(5)
WX Cet	0.05826	0.05956(3)	0.0218(5)
HO Del	0.06266	0.06440(6)	0.0270(10)
XZ Eri	0.06116	0.06285(3)	0.0277(5)
AQ Eri	0.06094	0.06256(23)	0.0270(38)
V2051 Oph	0.06243	0.06426(5)	0.0285(8)
V1159 Ori	0.06218	0.06417(3)	0.0310(5)
V4140 Sgr	0.06143	0.06351(4)	0.0328(7)
QZ Vir	0.05882	0.06043(2)	0.0266(3)
SDSS J0903	0.05907	0.06036(5)	0.0213(8)
SDSS J1250	0.05874	0.06030(2)	0.0258(3)
SDSS J2048	0.06060	0.06166(2)	0.0172(3)
OT J105122	0.05960	0.06105(10)	0.0238(17)
OT J1706	0.05820	0.05946(7)	0.0211(12)
OT J2109	0.05865	0.06005(2)	0.0232(3)

$\ddagger$ Unit d.

$\dagger$ Fractional superhump excess (in frequency unit).

### 5.7. Evolutionary State

Table 12 lists fractional superhump excesses (in frequency unit) of WZ Sge-type dwarf novae with multiple rebrightenings (type-B). We find the 95% quantile of superhump periods of WZ Sge-type dwarf novae with multiple rebrightenings between 0.05875 and 0.06458 d (figure 15). In this period region, there are many SU UMa-type stars without a rebrightening. We therefore make a comparison between them and WZ Sge-type dwarf novae with multiple rebrightenings. The fractional superhump excesses (in frequency unit) from stage A superhumps and stage B superhumps are also listed in table 13 and table 14, respectively.

Figure 16 and figure 17 show the relation between  $P_{\text{orb}}$  versus  $\epsilon^*$  for WZ Sge-type dwarf novae with multiple rebrightenings (listed in table 12) and SU UMa-type dwarf novae (listed in tables 13 and 14).

Figure 16 shows  $\epsilon^*$  from stage A superhumps of SU UMa-type dwarf novae without a rebrightening (filled circles) and WZ Sge-type dwarf novae with multiple rebrightenings (filled stars). Figure 17 shows  $\epsilon^*$  from stage B superhumps of SU UMa-type dwarf novae without a rebrightening (filled squares) and WZ Sge-type dwarf novae with multiple rebrightenings (filled triangles).

$\epsilon^*$  from stage A superhumps of WZ Sge-type dwarf novae with multiple rebrightenings are located in a region with a little smaller  $\epsilon^*$  than those of SU UMa-type dwarf novae without a rebrightening. Using the relation between  $\epsilon^*$  of stage A superhumps and  $q$  (subsection 5.3),  $q$  of WZ Sge-type dwarf novae with multiple rebrightenings are estimated close to (only slightly smaller than) those of SU UMa-type dwarf novae without a rebrightening. However, they are two different populations using  $\epsilon^*$  from stage B superhumps.  $\epsilon^*$  from stage B superhumps of WZ Sge-type dwarf novae with multiple rebrightenings are clearly smaller than that of SU UMa-type dwarf novae without a rebrightening.

Murray (2000) formulated the hydrodynamical precession  $\omega$  in the form:

$$\omega = \omega_{\text{dyn}} + \omega_{\text{pres}} \quad (10)$$

where  $\omega_{\text{dyn}}$  and  $\omega_{\text{pres}}$  are the dynamic precession and the pressure contribution to the precession.  $\omega_{\text{pres}}/\omega_{\text{orb}}$  corresponds to  $\epsilon_A^* - \epsilon_B^*$ , where  $\epsilon_A^*$  and  $\epsilon_B^*$  are  $\epsilon^*$  from stage A and that of stage B, respectively.  $\epsilon_A^* - \epsilon_B^*$  is generally similar between those two types of systems. It is shown that  $\epsilon_A^* - \epsilon_B^* \simeq 0.010$  in SU UMa-type dwarf novae without a rebrightening and  $\simeq 0.015$  in WZ Sge-type dwarf novae with multiple rebrightenings.

We consider two possible interpretations of this result of great interest. The first interpretation,  $q$  from stage B superhumps is indeed the case and that  $q$  from stage A does not reflect the true  $q$ . The second interpretation,  $q$  from stage B superhumps does not reflect the true  $q$ . If the former interpretation is correct, the small  $q$  of WZ Sge-type dwarf novae with multiple rebrightenings suggest that the systems are good candidates for period bouncers. If the latter interpretation is the case, there is insignificant difference in  $q$  between WZ Sge-type dwarf novae

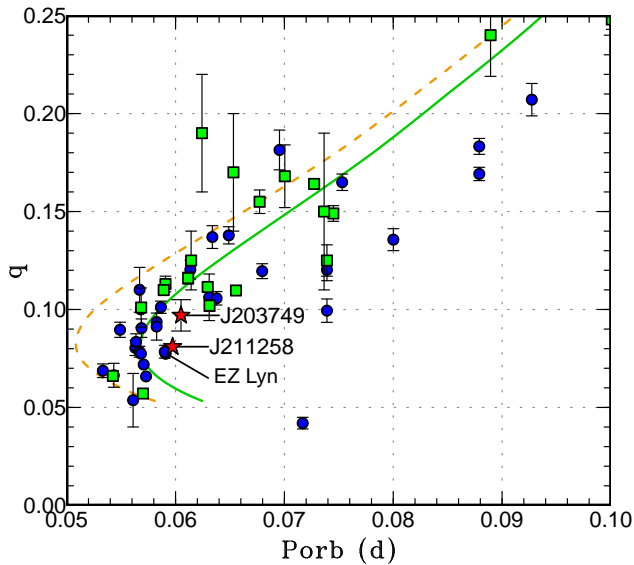


**Fig. 18.**  $q$  versus  $P_{\text{orb}}$ . The data are from Kato, Osaki (2013). The filled circles, filled squares and filled stars represent  $q$  from stage A superhumps,  $q$  measured by eclipse and our data ( $q$  from stage A superhumps), respectively. Our data are located in almost the same place as other SU UMa-type dwarf novae. The dash curved line and solid curved line represent evolutionary track of the standard evolutionary theory and that of the modified evolutionary theory (Knigge et al. 2011), respectively.

with multiple rebrightenings and SU UMa-type dwarf novae without a rebrightening. In the latter interpretation, small  $q$  from stage B superhumps may be explained as a result of a stronger pressure effect during stage B. These two possibilities should be tested by future studies. We, however, have no idea why growing superhumps arise from a radius other than the 3:1 resonance, and we are in favor of the latter interpretation.

Our result suggests a new picture that both classes of objects are located in the same place in the evolutionary trace (figure 18). The difference between these classes may be a result of different mass transfer rates. This possibility should be explored by future studies.

## 6. Summary

We obtained photometric observations of WZ Sge-type dwarf novae, MASTER OT J211258.65+242145.4 and MASTER OT J203749.39+552210.3 in 2012. The early superhumps with a period of 0.059732(3) d (MASTER J211258) and of 0.06050 d (MASTER J203749) were recorded. During superoutburst, ordinary superhumps with a period of 0.060291(4) d (MASTER J211258) and of 0.061307(9) d (MASTER J203749) were observed. The  $O-C$  curve clearly showed the presence of stage A and stage B. Both dwarf novae exhibited multiple rebrightenings after the main superoutburst.

In both dwarf novae, the increase of brightness were seen during the evolutionary stage of ordinary superhumps. Compared with other systems showing this phenomenon, we can see a possible tendency that those systems exhibit long rebrightening or multiple rebrightenings.

From the distribution of superhump periods, those superhump periods of type-B stars are systematically longer than those of type-D stars.

We estimated binary mass ratios by a new method using the period of superhumps in SU UMa-type dwarf novae during stage A superhumps. The method gave higher mass ratios for these objects than those from stage B superhumps by the traditional method. This suggests that the stage B superhump period is shorter due to effects of gas pressure. This result leads to a different picture of the evolutionary state in WZ Sge-type dwarf novae with multiple rebrightenings although they have been expected to be good candidates for period bouncers due to the small mass ratios expected from the period of stage B superhumps.

In the final part of the superoutburst, the increase in the superhump periods was seen in both systems. We presented an interpretation that the increase in the superhump periods is a result of the decrease of pressure effect during the final stage of the superoutburst and showed that the derived disk radius is in fair agreement with the previous work.

We acknowledge with thanks the variable star observations from the AAVSO International Database contributed by observers worldwide and used in this research. This work is deeply indebted to outburst detections and quick announcement by the MASTER network. We are grateful to many amateur observers.

## References

- Bailey, J. 1979, MNRAS, 189, 41P
- Balanutsa, P., et al. 2012, Astron. Telegram, 4515
- Buat-Ménard, V., & Hameury, J.-M. 2002, A&A, 386, 891
- Cleveland, W. S. 1979, J. Amer. Statist. Assoc., 74, 829
- Denisenko, D., et al. 2012, Astron. Telegram, 4208
- Downes, R. A. 1990, AJ, 99, 339
- Fernie, J. D. 1989, PASP, 101, 225
- Gorbovskoy, E. S., et al. 2013, Astron. Rep., 57, 233
- Hameury, J.-M. 2000, New Astron. Rev., 44, 15
- Huruhata, M. 1983, IBVS, 2401
- Imada, A., Kubota, K., Kato, T., Nogami, D., Maehara, H., Nakajima, K., Uemura, M., & Ishioka, R. 2006, PASJ, 58, L23
- Ishioka, R., Uemura, M., Kato, T., & The VSNET Collaboration Team 2002a, in ASP Conf. Ser. 261, The Physics of Cataclysmic Variables and Related Objects, ed. B. T. Gänsicke, K. Beuermann, & K. Reinsch (San Francisco: ASP), p. 491
- Ishioka, R., Uemura, M., Kato, T., & The VSNET Collaboration Team 2002b, in ASP Conf. Ser. 261, The Physics of Cataclysmic Variables and Related Objects, ed. B. T. Gänsicke, K. Beuermann, & K. Reinsch (San Francisco: ASP), p. 489



- Ishioka, R., et al. 2002c, *A&A*, 381, L41  
Kato, T. 2002, *PASJ*, 54, L11  
Kato, T., et al. 2013a, *PASJ*, 65, 23  
Kato, T., et al. 2009a, *PASJ*, 61, S395  
Kato, T., et al. 2012, *PASJ*, 64, 21  
Kato, T., et al. 2010, *PASJ*, 62, 1525  
Kato, T., Monard, B., Hamsch, F.-J., Kiyota, S., & Maehara, H. 2013b, *PASJ*, in press (arXiv astro-ph/1307.5936)  
Kato, T., Nogami, D., Baba, H., Matsumoto, K., Arimoto, J., Tanabe, K., & Ishikawa, K. 1996, *PASJ*, 48, L21  
Kato, T., Nogami, D., Matsumoto, K., & Baba, H. 2004, *PASJ*, 56, S109  
Kato, T., & Osaki, Y. 2013, *PASJ*, in press (arXiv astro-ph/1307.5588)  
Kato, T., et al. 2009b, *PASJ*, 61, 601  
Kato, T., Sekine, Y., & Hirata, R. 2001, *PASJ*, 53, 1191  
Knigge, C., Baraffe, I., & Patterson, J. 2011, *ApJS*, 194, 28  
Kuulkers, E., Howell, S. B., & van Paradijs, J. 1996, *ApJL*, 462, L87  
Littlefair, S. P., Dhillon, V. S., Marsh, T. R., Gänsicke, B. T., Southworth, J., Baraffe, I., Watson, C. A., & Copperwheat, C. 2008, *MNRAS*, 388, 1582  
Lubow, S. H. 1991, *ApJ*, 381, 259  
Lubow, S. H. 1992, *ApJ*, 398, 525  
Matsumoto, K., & Schmeer, P. 1996, *IAU Circ.*, 6517  
Mroz, P., et al. 2013, *Acta Astron.*, in press (arXiv astro-ph/1307.1238)  
Murray, J. R. 2000, *MNRAS*, 314, 1P  
Nakagawa, S., Noguchi, R., Iino, E., Ogura, K., Matsumoto, K., Arai, A., Isogai, M., & Uemura, M. 2013, *PASJ*, 65, 70  
Nogami, D., Kato, T., Baba, H., Matsumoto, K., Arimoto, J., Tanabe, K., & Ishikawa, K. 1997, *ApJ*, 490, 840  
Osaki, Y. 1995, *PASJ*, 47, 47  
Osaki, Y. 1996, *PASP*, 108, 39  
Osaki, Y., & Kato, T. 2013, *PASJ*, in press (arXiv astro-ph/1305.5877)  
Osaki, Y., & Meyer, F. 2002, *A&A*, 383, 574  
Osaki, Y., & Meyer, F. 2003, *A&A*, 401, 325  
Osaki, Y., Meyer, F., & Meyer-Hofmeister, E. 2001, *A&A*, 370, 488  
Osaki, Y., Shimizu, S., & Tsugawa, M. 1997, *PASJ*, 49, L19  
Patterson, J. 2011, *MNRAS*, 411, 2695  
Patterson, J., Augusteijn, T., Harvey, D. A., Skillman, D. R., Abbott, T. M. C., & Thorstensen, J. 1996, *PASP*, 108, 748  
Patterson, J., et al. 2005a, *PASP*, 117, 1204  
Patterson, J., et al. 1998, *PASP*, 110, 1290  
Patterson, J., McGraw, J. T., Coleman, L., & Africano, J. L. 1981, *ApJ*, 248, 1067  
Patterson, J., et al. 2002, *PASP*, 114, 721  
Patterson, J., Thorstensen, J. R., & Kemp, J. 2005b, *PASP*, 117, 427  
Pavlenko, E., et al. 2007, in *ASP Conf. Ser.* 372, 15th European Workshop on White Dwarfs, ed. R. Napiwotzki, & M. R. Burleigh (San Francisco: ASP), p. 511  
Stellingwerf, R. F. 1978, *ApJ*, 224, 953  
Thorstensen, J. R., Fenton, W. H., Patterson, J. O., Kemp, J., Halpern, J., & Baraffe, I. 2002, *PASP*, 114, 1117  
Uemura, M., et al. 2008, *IBVS*, 5815, 1  
Uemura, M., Kato, T., Nogami, D., & Ohsugi, T. 2010, *PASJ*, 62, 613